








## Article

# Syngas Quality in Fluidized Bed Gasification of Biomass: Comparison between Olivine and K-Feldspar as Bed Materials

Beatrice Vincenti <sup>1,2</sup>, Francesco Gallucci <sup>1,\*</sup>, Enrico Paris <sup>1,2</sup>, Monica Carnevale <sup>1</sup>, Adriano Palma <sup>1</sup>, Mariangela Salerno <sup>1</sup>, Carmine Cava <sup>2</sup>, Orlando Palone <sup>2</sup>, Giuliano Agati <sup>2</sup>, Michele Vincenzo Migliarese Caputi <sup>2</sup> and Domenico Borello <sup>2</sup>

<sup>1</sup> Council for Agricultural Research and Economics (CREA), 00015 Rome, Italy

<sup>2</sup> Department of Mechanical and Aerospace Engineering, La Sapienza University of Rome, 00185 Rome, Italy

\* Correspondence: francesco.gallucci@crea.gov.it

**Abstract:** The relevance of selecting an appropriate bed material in fluidized bed gasification is a crucial aspect that is often underestimated. The ideal material should be economical, resistant to high temperatures and have small chemical interaction with biomass. However, often only the first of such three aspects is considered, neglecting the biomass–bed interaction effects that develop at high temperatures. In this work, olivine and K-feldspar were upscale-tested in a prototype fluidized bed gasifier (FBG) using arboreal biomass (almond shells). The produced syngas in the two different tests was characterized and compared in terms of composition (H<sub>2</sub>, CH<sub>4</sub>, CO, CO<sub>2</sub>, O<sub>2</sub>) and fate of contaminants such as volatile organic compounds (VOCs), tar and metals. Moreover, the composition of olivine and K-feldspar before and after the biomass gasification process has been characterized. The aim of this work is to show which advantages and disadvantages there are in choosing the most suitable material and to optimize the biomass gasification process by reducing the undesirable effects, such as heavy metal production, bed agglomeration and tar production, which are harmful when syngas is used in internal combustion engines (ICE). It has been observed that metals, such as Ni, Cu, Zn, Cd, Sn, Ba and Pb, have higher concentrations in the syngas produced by using olivine as bed material rather than K-feldspar. In particular, heavy metals, such as Pb, Cu, Cd, Ni and Zn, show concentrations of 61.06 mg/Nm<sup>3</sup>, 15.29 mg/Nm<sup>3</sup>, 17.97 mg/Nm<sup>3</sup>, 37.29 mg/Nm<sup>3</sup> and 116.39 mg/Nm<sup>3</sup>, respectively, compared to 23.26 mg/Nm<sup>3</sup>, 11.82 mg/Nm<sup>3</sup>, 2.76 mg/Nm<sup>3</sup>, 24.46 mg/Nm<sup>3</sup> and 53.07 mg/Nm<sup>3</sup> detected with K-feldspar. Moreover, a more hydrogen-rich syngas when using K-feldspar was produced (46% compared to 39% with olivine).

**Keywords:** fluidized bed gasification; K-feldspar; olivine; syngas; bed material; biomass; almond shells; metals; tar; VOCs



**Citation:** Vincenti, B.; Gallucci, F.; Paris, E.; Carnevale, M.; Palma, A.; Salerno, M.; Cava, C.; Palone, O.; Agati, G.; Caputi, M.V.M.; et al. Syngas Quality in Fluidized Bed Gasification of Biomass: Comparison between Olivine and K-Feldspar as Bed Materials. *Sustainability* **2023**, *15*, 2600. <https://doi.org/10.3390/su15032600>

Academic Editor: Marc A. Rosen

Received: 10 October 2022

Revised: 2 January 2023

Accepted: 29 January 2023

Published: 1 February 2023



**Copyright:** © 2023 by the authors. Licensee MDPI, Basel, Switzerland. This article is an open access article distributed under the terms and conditions of the Creative Commons Attribution (CC BY) license (<https://creativecommons.org/licenses/by/4.0/>).

## 1. Introduction

The increase in global energy demand, along with climate change threats and geopolitical instability that affect fossil fuel availability, have shifted energy demand toward renewable energy sources [1,2]. Compared to traditional fossil fuels, biomass is broadly available and produces a lower impact on the environment [3]. The production of energy from biomass solves some fundamental problems affecting other forms of renewable energy, such as wind and solar energy, as complex storage and the ability to produce energy when needed [4,5]. Easy to store, biomass guarantees continuity of supply and availability of energy, and its negligible sulfur content along with highly volatile components of most types of lignocellulosic biomass increase the benefits of its use in gasification processes [6,7]. Gasification represents a promising technology for converting biomass into a fuel source [8–11]. Through a series of chemical reactions, gasification leads to the production of a synthetic gas, the so-called syngas [12–14], which possesses a larger energy density than biomass and can be used in many applications, including fuel cell power generation, internal combustion

engines (ICE) or gas turbines [15,16] After properly cleaned of ashes and tar (a complex mixture of condensable hydrocarbons), syngas is mostly composed of carbon monoxide (CO), carbon dioxide (CO<sub>2</sub>), hydrogen (H<sub>2</sub>) and methane (CH<sub>4</sub>) besides nitrogen (N<sub>2</sub>) in the case of air or enriched air as an oxidant carrier agent [3,17].

Fluidized bed gasification (FBG) is a widely commercialized technology for converting biomass into a fuel source. One key advantage of FBG is the ability to maintain a constant bed temperature using bubbling beds composed of a mixture of biomass and materials, such as olivine, K-feldspar, quartz sand or sepiolite. [18], which act as thermal energy carriers and mixers [19]. The selection of appropriate bed material gives benefit to the process in terms of heat transfer, mass transfer and fuel mixing so as to allow the reactor to maintain an isothermal behavior and high performance. Thus, by means of a thoughtful selection of suitable minerals, bed properties can be evaluated in order to optimize the gasification process and increase the syngas quality by facilitating biomass conversion and guaranteeing limited contents of undesirable products such as tar and alkali compounds. The optimal materials to employ are determined by chemical, mechanical and environmental considerations. However, too frequently, the mechanical and economic factors are prioritized above the chemical consequences that inevitably lead to affecting the quality of the syngas. Several research works have focused on the importance of the study of chemical reactions occurring in gasifiers with the aim of obtaining a syngas with the lowest concentration of pollutants [15], while there is a lack of study about the interaction that occurs between the different bed materials and the selected biomass. Some authors found that tar decreased while H<sub>2</sub> production increased due to improved steam reforming and water–gas shift reactions in fluidized beds where olivine served as bed material [20,21]. Different materials were also tested, e.g., Soria-Verdugo et al. 2019 [22] conducted research focused on studying the gasification process of a lignocellulosic biomass in a bubbling fluidized gasifier. Sepiolite, a lower particle density material, was tested, and a larger H<sub>2</sub> production together with a lower tar concentration were found. With regard to the reduction of metal emissions, many studies have proposed various strategies that involved the assessment of the bed and the materials that constitute it [23–25].

In previous works [26,27], some of the most commonly used materials in the literature (i.e., olivine, K-feldspar, calcite and kaolinite [28,29]) were lab-scale-tested in order to establish which minerals were the most suitable for the bed constitution. Tests were conducted in TGA-DSC (thermogravimetric and differential scanning calorimetry analysis) that proved to be an excellent lab-scale approximation for the evaluation of syngas produced from a fluidized bed gasificator [26], with a few milligrams of material combined with a few milligrams of arboreal or herbaceous biomass obtained from plant-assisted bioremediation (PABR) processes [30], with the aim to determine which material of the bed provided better performance in terms of less heavy metal syngas contamination. It turned out that K-feldspar was the most versatile material, with optimal results with both arboreal and herbaceous PABR biomass, while olivine provided good results only with arboreal PABR biomass. This research work represents a step forward in the assessment of such an analysis: results previously obtained were used as a basis for operating on a real prototypal plant of fluidized bed gasification, in which the best-performing materials in a lab-scale test, olivine (O) and K-feldspar (K), have been compared using almond shells which, although not obtained from PABR processes, are an arboreal biomass widely available in large quantities. By means of a pilot scale FBG system, this research study aims to upgrade previous works with the purpose of providing a solid foundation for the selection of the best bed material in accordance with the type of biomass used to build an FBG plant, which yields a hydrogen-rich syngas with the fewest contaminants released by the biomass-bed interaction.

## 2. Materials and Methods

The gasification tests, the preliminary analysis as well as the instrumental measurements were all performed at LASER-B (Laboratory for Experimental Activities on Renewable Energy from Biomass) located at CREA-IT (Council for Agricultural Research

and Economic—department of Engineering and Agri-food transformations) in Monterotondo (Italy).

### 2.1. Biomass and Bed Materials Characterization

Almond shells (not obtained from PABR) were subjected to chemical–physical analysis in order to determine moisture and ash content, lower heating value (LHV), higher heating value (HHV) and elemental composition in terms of C, H, N and S. Preliminarily, the biomass was ground with a RetschSM 100 knife mill and then dried with a Memmert UFP800 oven at  $105 \pm 2$  °C for 24 h. The moisture content was determined in accordance with EN ISO 18134-1:(2015). The ash content was determined in accordance with EN ISO 18122:(2015): about one gram of biomass was placed in a muffle furnace (Lenton EF/11 8B) and first heated up to 250 °C for two hours with a 6.5 °C/min ramp and then up to 550 °C for one hour with a 10 °C/min ramp. HHV was determined in accordance with EN ISO 18125:(2009) using an Anton Paar 6400 isoperibolic calorimeter. Finally, LHV was obtained using the HHV and the hydrogen percentage.

The elemental analysis, allowing the determination of carbon, hydrogen, nitrogen and sulfur content, was measured in accordance with EN ISO 16848:(2015) using a Costech ECS 4010 CHNS-O elemental analyzer. About 5 mg of the sample was weighted into tin capsules and then placed into the reactor. The limit of quantification (LOQ) showed to be 0.05% w/w for each sample. The oxygen content was then determined by comparing dry samples (UNI EN ISO 16948:2015). All biomass characterization tests were conducted in duplicate.

Metal content was investigated both in biomass and in bed materials. Samples ( $\approx$  500 mg) were mineralized in acid environment using a microwave digester (Start D, Milestone, Italy) in order to make the sample suitable for introduction into an inductively coupled plasma mass spectrometer (ICP-MS) system (Agilent 7700). A solution for the acid composed of 6 mL of HNO<sub>3</sub> (65% v/v) and 3 mL of H<sub>2</sub>O<sub>2</sub> (30% v/v) was used for the acid attack and the sample solubilization. The instrument was calibrated using multi-element standards (Standard mix, concentration 10 ppm in metal, Ultrascientific) in an acidified aqueous solution (HNO<sub>3</sub> 2% v/v). The calibration line was developed with four standards ranging in concentration from 50 to 1000 ppb. Yttrium was employed as the internal standard via the instrument's automated input mechanism.

### 2.2. FBG Plant and Syngas Sampling

The gasification experiments were performed at CREA-IT in the fluidized bed gasifier (1 kW<sub>th</sub>) facility held by DIMA (Department of Mechanical and Aerospace Engineering—Sapienza University of Rome), previously adopted and described in recent studies [31,32]. The gasification plant used is shown in Figure 1. Olivine and K-feldspar selected as bed materials were sieved to ensure a granulometry between 100 and 200  $\mu$ m. For each test, 1 kg of bed material was used. The density of bed materials was 3.49 g/cm<sup>3</sup> for olivine and 2.77 g/cm<sup>3</sup> for K-feldspar. The system operated at constant (atmospheric) pressure, with a small overpressure in the fluidized bed of about 200 mbar (20 kPa). After being preheated in a wind box, air was sent into the FBG from the bottom side of the reactor with a mass flow rate adequate to generate a bubbling bed as well as to feed the gasifier with a sufficient quantity of oxygen required to support the gasification reactions (Table 1) [33]. In agreement with [34], reactor temperature was set at 820 °C. A LabView® application was used to control oxidant agent flow (air) by means of a mass-flow controller (Bronkhorst MFC 50 L/min). A Bronkhorst MFC calibrated for syngas flow rates ranging from 8 to 400 Nml/min was used to compute the syngas slipstream sent to the metals, tar and VOC sampling systems shown below.

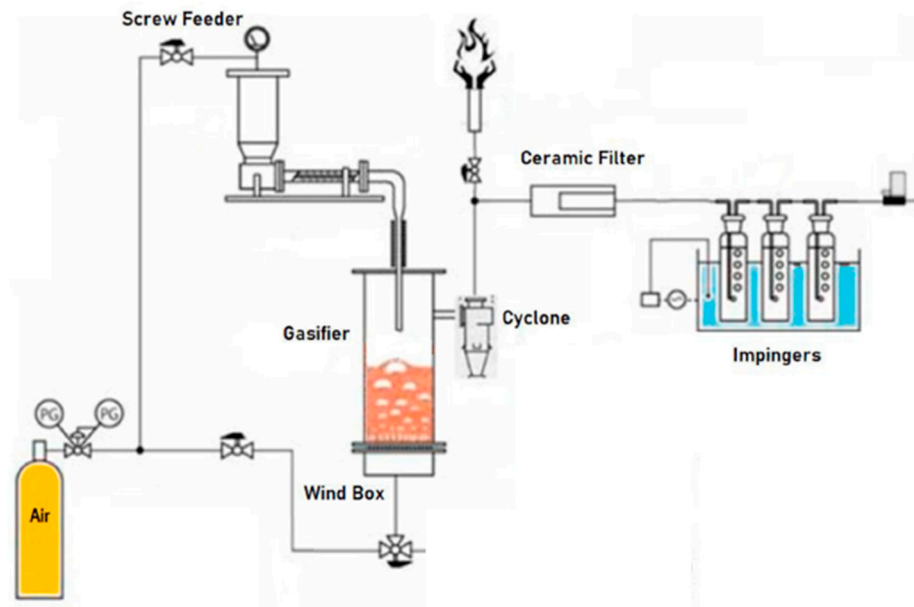


**Figure 1.** Schematic diagram of the gasification plant.

**Table 1.** Operating conditions in the FBG.

Air [Nl/min]	8
Wind box [°C]	450
Reactor [°C]	820
Biomass [g/h]	780
Equivalent ratio	0.3
Minimal fluidization velocity: olivine tests [m/s]	0.055
Minimal fluidization velocity: K-feldspar tests	0.044

The biomass was introduced into FBG through a screw fed by an electric motor and supplied by a tank. It was chosen to condition the system before the start of the sampling test to ensure a correct temperature distribution. In particular, tests were started about an hour after the achievement of the operating temperatures. The reaction time was about 1 h. The reaction was conducted for the time strictly necessary for the conditioning of the plant and the sampling phase. A pipe placed in the top region allows the produced syngas to be delivered to the cleaning section. On the contrary, the majority of char and ashes remain trapped in the reactor and mix with the bed material. The syngas purification section consists of a cyclone that removes the biggest char and ash fractions carried by the gas flow and a ceramic filter that heats the gas to 400 °C to promote thermal degradation of heavy compounds while preventing tar deposits. Finally, syngas passes into the final impingers system for fugitive ashes, tar and metals. A mass flow controller has been placed downstream from the impingers system, which allows recording the flow of syngas that has passed through the sampling system. The ashes present on the bottom of the reactor (bottom ashes) and those separated by the cyclone (flying ashes) were also collected and analyzed to determine the metal content. Syngas was collected using Tedlar<sup>®</sup> bags after the ceramic filter and subsequently characterized with a 3000 Micro GC Inficon gas analyzer in order to obtain the syngas composition on a dry basis. Bottom ashes are the heaviest fraction and are collected and mixed with char in the lower part of the gasifier. Hence, the presence and potential interaction of such components with the bed materials must be considered during analysis. Flying ashes are easily transported by the generated syngas and captured by the cyclone. Fugitive ashes, lastly, are caught by the trapping system consisting of the three impingers placed downstream of the ceramic filter.

It is possible to analyze the bottom ash deposit by comparing the metal contents of the reactor after the conclusion of the gasification with the material employed as a bed and,

equally important, the possible release of volatile metals from the bed materials and the successive transport in the syngas.

### 2.3. Metals and Tar Sampling and Analysis

The produced syngas was sampled in order to evaluate the metals and tar presence. A system of three impingers (250 mL, DadoLab) was set up in line and immersed in a thermostatic bath at sub-ambient temperature ( $5 \pm 1$  °C, DadoLab Chiller SC5). Syngas was bubbled inside the impingers each filled with 100 mL of a suitable solution for sampling the analytes. A solution of HNO<sub>3</sub> and H<sub>2</sub>O<sub>2</sub> in milli-Q water was used for the metals' sampling. This solution has a content of HNO<sub>3</sub>  $\approx$  3.3% v/v and H<sub>2</sub>O<sub>2</sub>  $\approx$  1.5% v/v, according to UNI EN 14385. Tar was sampled by bubbling the syngas in the same way in a  $\approx$  50% isopropanol solution. The third impinger, in both cases, is defined as *backup* and is used to check that the sampling was quantitative. A correct sampling requires that the concentration of the analytes in the third impinger does not exceed 5% compared to the sum of the same in the first two impingers. The impingers were placed at sub-ambient temperature in a thermal bath at 5 °C, to favor the trapping efficiency. The bubbled solutions were analyzed with the ICP-MS described above to determine the concentrations of the metal species, while the collected tar solutions were injected into a gas chromatograph coupled with a mass spectrometer (GC-MS) system (Agilent 7000). All experiments were carried out in duplicate.

### 2.4. VOCs Sampling and Analysis

Volatile organic compounds were also collected downstream of the gasifier. A sampling ATA (Air toxic analyzer, Markes Int.) was used in order to capture VOCs produced during the gasification process. Samplings were carried out by placing the adsorbent tubes in correspondence with the gasifier's gas outlet. Active sampling of the syngas was carried out at a flow of 50 mL/min using an appropriate sampling pump. All tests were conducted in duplicate. A thermal desorber 100-XR (TD, Markes Int.) was used for the analysis, carried out with an Agilent 7000 GC-MS system. Tubes were desorbed according to the method described by Paris et al. [35]. The GC-MS analysis was conducted according to the protocol outlined in Table 2, in splitless. The acquisition of volatile organic compounds (VOCs) was executed utilizing the full-scan mode within the mass-to-charge ratio range of 35-450 utilizing an electron ionization (EI) source at a temperature of 250 °C [35].

**Table 2.** GC ramp.

	Rate [°C/min]	T [°C]	Hold Time [min]
Initial	-	35	3
Ramp	5	250	5

## 3. Results and Discussion

### 3.1. Biomass Characterization

Almond shells were subjected to a physical–chemical characterization in order to evaluate their characteristics and their potential use as feedstock in biomass gasification processes. The elementary analysis carried out on almond shells showed the opportunity to use such biomass in thermochemical processes because of the C/N ratio higher than 30 and the moisture content equal to 10.36% [26]. The sulfur content was not quantifiable, hence it was not considered in the present analysis. Table 3 shows the results of such analysis.

**Table 3.** Physico–chemical characterization of almond shells used as fuel.

Parameter	Amount	Units
moisture	10.36	%
C	45.09	%
H	9.88	%
N	0.79	%
ash	4.61	%
HHV	20.37	MJ/kg
LHV	18.34	MJ/kg

### 3.2. Metal Assessment in Biomass and in Bed Materials

Results of ICP-MS analyses on biomass are presented as follows (Table 4). Bold values refer to relevant heavy metals. High concentrations of macroelements (Na, Mg, Ca, K) are attributable to the ability of the plant itself to assimilate such cationic species from the soil during the growing phase.

**Table 4.** Metals concentrations in almond shells.

Metal	mg/kg
Li	0.42
B	7.40
Na	91.72
Mg	19.79
Al	21.90
K	79.09
Ca	49.51
Cr	0.69
<b>Mn</b>	0.78
<b>Fe</b>	73.98
<b>Co</b>	0.62
Ni	2.14
Cu	2.05
Zn	4.06
Ag	0.13
Cd	0.12
<b>Sn</b>	8.09
Ba	1.15
<b>Pb</b>	0.47

A preliminary characterization of both bed materials selected for this study was conducted in a previous work [31]. Olivine showed a noticeable amount of Fe, Cr, Mn, Co and Ni, while K-feldspar contained large amounts of Ca, K and Al. Due to their catalytic effect, the presence of Ni and Fe can positively influence the gasification process and prevent tar formation [19]. Results obtained in such previous works are shown in Table 5.

**Table 5.** Metal content in bed materials [31].

mg/kg	Olivine	K-Feldspar	mg/kg	Olivine	K-Feldspar
Li	0.100	0.002	<b>Fe</b>	4508	15.82
B	0.01	0.01	<b>Co</b>	7.99	0.03
Na	12.72	2.97	Ni	149.9	0.37
Mg	17620.	2.80	Cu	1.55	0.05
Al	144.4	22.87	Zn	0.86	1.59
K	1.82	23.82	Ag	0.001	0.031
Ca	32.44	67.49	Cd	0.002	0.003
Cr	14.38	0.05	Ba	0.032	0.16
<b>Mn</b>	69.74	1.87	<b>Pb</b>	0.003	0.88

### 3.3. Metals in Bottom and Fly Ashes

The distribution of pollutants generated by the gasification process is extremely important to assess a correct disposal and separation procedure. Metals are concentrated in ash which may be distinguished into three fractions: bottom, flying and fugitive ashes, based on the stream they depend on. In Tables 6 and 7, metal concentrations in the flying and in the bottom ashes in both two different FBG systems (olivine + almond shells (OA) and K-feldspar + almond shells (KA)) are reported. When olivine was used as a boiling bed material, only four metals (Cr, Ni, Ag and Pb) remained confined within the bottom ashes rather than being transported by syngas in fly ashes. Metals dragged by the volatile fraction are Mg, Mn, Fe and Ca, whose concentrations in fly ashes are higher than 1 g/Kg. In the KA case, several metals, such as Li, Mg, Al, Fe, Co, Cu, Zn and Ag, are observed in higher concentrations in bottom ashes rather than in fly ashes. In KA tests, fly ashes are rich in K and Ca with concentrations above 1 g/kg, but unlike OA, no high concentrations of Mn and Fe in this ash fraction were detected. This comparison suggests that the high presence of Ca is probably due to biomass rather than bed material, while the contamination of syngas and ash with Mn and Fe is a consequence of the use of olivine as bed material. The comparison also shows that, generally, the KA combination leads to lower metal concentrations in the bottom and fly ashes than OA; this is due to the use of olivine which has a higher concentration of metals. The most volatile metals in the last ash fraction (*fugitive ashes*) were subsequently treated in a dedicated paragraph because their sampling method relates their concentrations to the amount of syngas (mg/Nm<sup>3</sup>) and not to the concentration of mg/kg ash. In fact, while for the bottom and fly ash, both separation and sampling are physical. In fugitive, the sampling is chemical and is necessarily related to the volume of syngas that has passed through the impingers.

**Table 6.** Metal content in olivine–almond shells system (bottom and fly ashes).

mg/kg	OA Bottom Ashes	OA Fly Ashes
Li	0.48	12.01
B	1.07	63.47
Na	210.4	532.6
Mg	98.91	52,960
Al	63.42	6561
K	122.9	6703
Ca	50.61	11,050
Cr	11,040	4423
Mn	1.79	16,900
Fe	29.21	48,720
Co	0.42	1591
Ni	32,490	7208
Cu	0.77	959.5
Zn	2.56	228.9
Ag	0.16	<LOQ
Cd	0.26	1.27
Sn	1.67	12.04
Ba	1.05	88.08
Pb	0.36	<LOQ

**Table 7.** Metal content in K-feldspar–almond shells system (bottom and fly ashes).

Mg/kg	KA Bottom Ashes	KA Fly Ashes
Li	0.69	<LOQ
B	3.62	123.4
Na	228.6	1602
Mg	18,390	4025
Al	146	<LOQ
K	537.9	24,050
Ca	334.2	17,350
Cr	153.3	2099
Mn	162.4	499.0
Fe	4368	1637
Co	17.66	<LOQ
Ni	1924	4169
Cu	2.60	1.41
Zn	3.62	<LOQ
Ag	0.24	<LOQ
Cd	0.11	1.76
Sn	<LOQ	<LOQ
Ba	5.83	272.2
Pb	<LOQ	<LOQ

### 3.4. Metals in Fugitive Ashes

Metals in fugitive ashes are the fraction not stored in the bottom ash of the reactor and not removed from the abatement systems, thus representing the fraction contained in the final syngas. In Table 8, it is observed that, in the OA tests, metals in the fugitive ashes are in greater concentrations compared to those obtained in the KA tests. This is in line with what was observed for the bottom and fly ashes, where even in that case olivine was found to be the most “contaminating” material during the gasification process and is also consistent with what has been observed in Table 6, where it is shown that olivine has higher metal concentrations.

**Table 8.** Metals in the fugitive ashes in the two different systems.

mg/Nm <sup>3</sup>	OA	KA
Li	<LOQ	<LOQ
B	<LOQ	<LOQ
Na	138.0	491.9
Mg	758.8	92.57
Al	<LOQ	<LOQ
K	1457	178.0
Ca	163.5	117.5
Cr	<LOQ	2.08
Mn	77.78	1.11
Fe	542.7	100.1
Co	<LOQ	<LOQ
Ni	37.29	24.46
Cu	15.29	11.82
Zn	116.4	53.07
Ag	<LOQ	<LOQ
Cd	17.97	2.76
Sn	84.44	19.42
Ba	119.2	86.99
Pb	61.06	23.26

The following data allow drawing important considerations in comparison with the previous lab-scale work. In particular, heavy metals present in greater quantities were Fe, Cu, Zn, Sn, Ni, Cd and Pb. Olivine showed worse performance in emission for Fe, Zn and



Sn as is also confirmed in upscale tests. The presence of Ni was similar in emission with both olivine and K-feldspar, while Pb, Cu and Cd had slightly higher concentrations in K-feldspar tests. These data have been confirmed only partially in the upscale test: the concentration of Ni is similar in both cases, but the concentrations of the other metals (Pb, Cu and Cd) are in contrast with the observed ones. This suggests that the K-feldspar has better performance on a prototype scale. The composition of Cr follows that observed in the lab-scale, as it has a higher concentration in the syngas produced using K-feldspar as bed material.

### 3.5. Syngas Characterization

Syngas compositions were analyzed to evaluate the best performance obtained between the use of the bed based on olivine or K-feldspar. As can be seen in Table 9, the use of K-feldspar led to a greater production of molecular hydrogen and methane than the system that used olivine. Data are normalized by excluding nitrogen percentage.

**Table 9.** Compounds expressed in % of the parameters analyzed in the syngas.

%	OA	KA
CO <sub>2</sub>	6	8
H <sub>2</sub>	39	46
O <sub>2</sub>	2	1
CH <sub>4</sub>	10	3
CO	42	43

### 3.6. Tar and VOCs Analysis

The results of the tar analysis are summarized in Table 10. The organic pollutant formation is probably favored by the catalytic effect of metals present on the bed material particle surface. The quantities of naphthalene, acenaphthylene and acenaphthene are similar in both processes, while in the case of the use of K-feldspar a higher concentration of Benzo[b]-fluoranthene was observed. It can be assumed that such material at FBG operating temperatures favors the formation of this compound compared to the other isomer observed (Benzo[k]-fluoranthene), which is in lower concentrations than in the case of olivine.

**Table 10.** Tar identified in the syngas produced in the two different systems.

µg/Nm <sup>3</sup>	OA	KA
Naphtalene	0.14	0.14
Acenaphthylene	<LOQ	<LOQ
Acenaphthene	0.47	0.48
Fluorene	<LOQ	<LOQ
Phenanthrene	<LOQ	<LOQ
Anthracene	<LOQ	<LOQ
Fluoranthene	<LOQ	<LOQ
Pyrene	<LOQ	<LOQ
Benzo[a]anthracene	0.17	0.06
Chrysene	<LOQ	<LOQ
Benzo[b]fluoranthene	16.79	314.04
Benzo[k]fluoranthene	3.51	<LOQ
Benzo[e]pyrene	37.11	27.01
Benzo[a]pyrene	19.18	12.06
Perylene	185.3	139.2
Benzo[ghi]perylene	<LOQ	<LOQ

VOC analysis in the syngas provided the results shown in Table 11, where the 10 quantifiable compounds of the approximately 30 compounds identified using the analytical standards are reported. Data are normalized to the volume, since each sampling was

conducted with an aspiration flow of 60 mL/min for 5 min for a total sample volume of 300 mL. There are no substantial differences between the OA and KA tests other than hexane and thiophene, which are found to be under the LOQ only in the OA case and only in the KA case, respectively. The similarity of the results could be partly justified by the fact that VOC sampling was conducted after syngas passed through the ceramic filter, which leads to a thermal cracking of larger organic molecules (tar) which are divided into structurally simpler compounds (VOCs) [26].

**Table 11.** Organic volatile compounds detected in the produced syngas from the two different systems.

mg/m <sup>3</sup>	OA	KA
Propane	0.43	1.51
Butane	0.46	0.81
Pentane	0.51	0.37
Hexane	<LOQ	0.33
1,5-Hexadiyne	18.58	19.99
Thiophene	6.36	<LOQ
Benzene	17.19	17.0
Toluene	12.72	11.65
m,p-Xylene	0.40	0.31
o-xylene	0.11	0.13

#### 4. Conclusions

The research study investigated the behavior of two of the most used bed materials in the FBG process of almond shells, an agroforestry by-product. This work is the upgrading in prototype scale of a previous lab-scale study in which four bed materials were compared with arboreal and herbaceous biomass to determine if during gasification contaminants are released into the syngas. From the previous study conducted in TGA-DSC emerged that K-feldspar was optimal for both arboreal and herbaceous biomass, while the olivine was optimal only for arboreal biomass. From the present analysis, it is clear that olivine is the one that tends most easily to contribute to the contamination of syngas in terms of heavy metals (such as Ni, Cu, Zn, Cd, Sn, Ba and Pb), while K-feldspar allows obtaining a cleaner syngas. An exception is represented by Cr, whose presence is detected only in tests carried out using K-feldspar. This data is in accordance with lab-scale tests. As for the organic contaminants tar and VOCs, there is no substantial difference between the two FBG bed materials used, except for Benzo[b]fluoranthene whose concentration in the syngas produced using K-feldspar is approximately 20 times higher than that detected using olivine. In conclusion, the behavior of such materials was again monitored in a pilot gasification plant using the arboreal biomass of almond shells which can then be used as a new energy source from a circular economy perspective. K-feldspar, besides being a minor metal emitter, shows a higher capacity in combination with biomass to produce a syngas richer in H<sub>2</sub>.

**Author Contributions:** Conceptualization, B.V., E.P. and D.B.; methodology, F.G. and D.B.; validation, A.P., M.C., M.S., C.C. and O.P.; investigation, B.V., E.P., M.C., A.P., C.C. and O.P.; data curation, G.A. and M.V.M.C.; writing—original draft preparation, B.V. and E.P.; writing—review and editing, F.G. and D.B.; supervision, D.B.; funding acquisition, F.G. All authors have read and agreed to the published version of the manuscript.

**Funding:** This work was supported by the Italian Minister of Agriculture, Food Sovereignty and Forests (MASAF) under the AGROENER (D.D. n. 26329, 01/04/2016) and sub-project “Tecnologie digitali integrate per il rafforzamento sostenibile di produzioni e trasformazioni agroalimentari (AgroFilire)” (AgriDigit programme), (DM 36503.7305.2018 of 20/12/2018).

**Institutional Review Board Statement:** Not applicable.

**Informed Consent Statement:** Not applicable.

**Data Availability Statement:** Not applicable.

**Conflicts of Interest:** The authors declare non conflict of interest.

## References

1. Paltsev, S. The complicated geopolitics of renewable energy. *Bull. At. Sci.* **2016**, *72*, 390–395. [[CrossRef](#)]
2. Franzitta, V.; Curto, D.; Rao, D.; Viola, A. Renewable energy sources to fulfill the global energy needs of a country: The case study of Malta in Mediterranean Sea. In Proceedings of the Ocean 2016, Shanghai, China, 10–13 April 2016; pp. 1–5. [[CrossRef](#)]
3. Cerone, N.; Zimbardi, F.; Contuzzi, L.; Baleta, J.; Cerinski, D.; Skvorčinskienė, R. Experimental investigation of syngas composition variation along updraft fixed bed gasifier. *Energy Convers. Manag.* **2020**, *221*, 113116. [[CrossRef](#)]
4. Anukam, A.; Goso, B.; Okoh, O.; Mamphweli, N. Studies on Characterization of Corn Cob for Application in a Gasification Process for Energy Production. *J. Chem.* **2017**, *2017*, 1–9. [[CrossRef](#)]
5. Abdelhady, S.; Borello, D.; Shaban, A. Techno-economic assessment of biomass power plant fed with rice straw: Sensitivity and parametric analysis of the performance and the LCOE. *Renew. Energy* **2018**, *115*, 1026–1034. [[CrossRef](#)]
6. Bridgwater, A.V. The technical and economic feasibility of biomass gasification for power generation. *Fuel* **1995**, *74*, 631–653. [[CrossRef](#)]
7. Sriram, N.; Shahidehpour, M. Renewable biomass energy. *IEEE Power Eng. Soc. Gen. Meet.* **2005**, *1*, 612–617. [[CrossRef](#)]
8. Di Gruttola, F.; Borello, D. Analysis of the EU Secondary Biomass Availability and Conversion Processes to Produce Advanced Biofuels: Use of Existing Databases for Assessing a Metric Evaluation for the 2025 Perspective. *Sustainability* **2021**, *13*, 7882. [[CrossRef](#)]
9. Pereira, E.G.; Da Silva, J.N.; De Oliveira, J.L.; MacHado, C.S. Sustainable energy: A review of gasification technologies. *Renew. Sustain. Energy Rev.* **2012**, *16*, 4753–4762. [[CrossRef](#)]
10. Sansaniwal, S.K.; Rosen, M.A.; Tyagi, S.K. Global challenges in the sustainable development of biomass gasification: An overview. *Renew. Sustain. Energy Rev.* **2017**, *80*, 23–43. [[CrossRef](#)]
11. Miccio, F.; Picarelli, A.; Ruoppolo, G. Increasing tar and hydrocarbons conversion by catalysis in bubbling fluidized bed gasifiers. *Fuel Process Technol.* **2016**, *141*, 31–37. [[CrossRef](#)]
12. Yang, S.; Wang, H.; Wei, Y.; Hu, J.; Chew, J.W. Numerical Investigation of Bubble Dynamics during Biomass Gasification in a Bubbling Fluidized Bed. *ACS Sustain. Chem. Eng.* **2019**, *7*, 12288–12303. [[CrossRef](#)]
13. Vargas-Salgado, C.; Hurtado-Pérez, E.; Alfonso-Solar, D.; Malmquist, A. Empirical Design, Construction, and Experimental Test of a Small-Scale Bubbling Fluidized Bed Reactor. *Sustainability* **2021**, *13*, 1061. [[CrossRef](#)]
14. Colantoni, A.; Longo, L.; Gallucci, F.; Monarca, D. Pyro-gasification of hazelnut pruning using a downdraft gasifier for concurrent production of syngas and biochar. *Contemp. Eng. Sci.* **2016**, *9*, 1339–1348. [[CrossRef](#)]
15. Di Carlo, A.; Borello, D.; Bocci, E. Process simulation of a hybrid SOFC/mGT and enriched air/steam fluidized bed gasifier power plant. *Int. J. Hydrog. Energy* **2013**, *38*, 5857–5874. [[CrossRef](#)]
16. Beheshti, S.M.; Ghassemi, H.; Shahsavan-Markadeh, R. An advanced biomass gasification–proton exchange membrane fuel cell system for power generation. *J. Clean. Prod.* **2016**, *112*, 995–1000. [[CrossRef](#)]
17. Farzad, S.; Mandegari, M.A.; Görgens, J.F. A critical review on biomass gasification, co-gasification, and their environmental assessments. *Biofuel Res. J.* **2016**, *3*, 483–495. [[CrossRef](#)]
18. Kuba, M.; Skoglund, N.; Öhman, M.; Hofbauer, H. A review on bed material particle layer formation and its positive influence on the performance of thermo-chemical biomass conversion in fluidized beds. *Fuel* **2021**, *291*, 120214. [[CrossRef](#)]
19. Gómez-Barea, A.; Ollero, P.; Leckner, B. Optimization of char and tar conversion in fluidized bed biomass gasifiers. *Fuel* **2013**, *103*, 42–52. [[CrossRef](#)]
20. Berdugo Vilches, T.; Marinkovic, J.; Seemann, M.; Thunman, H. Comparing Active Bed Materials in a Dual Fluidized Bed Biomass Gasifier: Olivine, Bauxite, Quartz-Sand, and Ilmenite. *Energy Fuels* **2016**, *30*, 4848–4857. [[CrossRef](#)]
21. Marinkovic, J.; Thunman, H.; Knutsson, P.; Seemann, M. Characteristics of olivine as a bed material in an indirect biomass gasifier. *Chem. Eng. J.* **2015**, *279*, 555–566. [[CrossRef](#)]
22. Soria-Verdugo, A.; Von Berg, L.; Serrano, D.; Hochenauer, C.; Scharler, R.; Anca-Couce, A. Effect of bed material density on the performance of steam gasification of biomass in bubbling fluidized beds. *Fuel* **2019**, *257*, 116118. [[CrossRef](#)]
23. Nowak, B.; Aschenbrenner, P.; Winter, F. Heavy metal removal from sewage sludge ash and municipal solid waste fly ash—A comparison. *Fuel Process Technol.* **2013**, *105*, 195–201. [[CrossRef](#)]
24. Lin, C.L.; Wu, M.H.; Weng, W.C. Effect of the type of bed material in two-stage fluidized bed gasification reactors on hydrogen gas synthesis and heavy metal distribution. *Int. J. Hydrog. Energy* **2019**, *44*, 5633–5639. [[CrossRef](#)]
25. Dastyar, W.; Raheem, A.; He, J.; Zhao, M. Biofuel Production Using Thermochemical Conversion of Heavy Metal-Contaminated Biomass (HMCB) Harvested from Phytoextraction Process. *Chem. Eng. J.* **2019**, *358*, 759–785. [[CrossRef](#)]
26. Gallucci, F.; Paris, E.; Palma, A.; Vincenti, B.; Carnevale, M.; Ancona, V.; Borello, D. Fluidized bed gasification of biomass from plant-assisted bioremediation: Fate of contaminants. *Sustain. Energy Technol. Assess.* **2022**, *53*, 102458. [[CrossRef](#)]
27. Borello, D.; De Caprariis, B.; Ancona, V.; Paris, E.; Plescia, P.; Gallucci, F. Use of an innovative TGA apparatus for sampling the emissions generated by pyrolysis of plant assisted bio-remediation biomass. In Proceedings of the European biomass conference and exhibition, Bologna, Italy, 5–8 June 2020; pp. 302–305.

28. Mauerhofer, A.M.; Benedikt, F.; Schmid, J.C.; Fuchs, J.; Müller, S.; Hofbauer, H. Influence of different bed material mixtures on dual fluidized bed steam gasification. *Energy* **2018**, *157*, 957–968. [[CrossRef](#)]
29. Wagner, K.; Häggström, G.; Skoglund, N.; Priscak, J.; Kuba, M.; Öhman, M.; Hofbauer, H. Layer formation mechanism of K-feldspar in bubbling fluidized bed combustion of phosphorus-lean and phosphorus-rich residual biomass. *Appl. Energy* **2019**, *248*, 545–554. [[CrossRef](#)]
30. Ancona, V.; Barra Caracciolo, A.; Campanale, C.; De Caprariis, B.; Grenni, P.; Uricchio, V.F.; Borello, D. Gasification treatment of poplar biomass produced in a contaminated area restored using plant assisted bioremediation. *J. Environ. Manage.* **2019**, *239*, 137–141. [[CrossRef](#)]
31. Gallucci, F.; Palma, A.; Vincenti, B.; Carnevale, M.; Paris, E.; Ancona, V.; Caputi, M.V.M.; Borello, D. Fluidized bed gasification of biomass from plant assisted bioremediation (PABR): Lab-scale assessment of the effect of different catalytic bed material on emissions. *Fuel* **2022**, *322*, 124214. [[CrossRef](#)]
32. Gallucci, F.; Liberatore, R.; Sapegno, L.; Volponi, E.; Venturini, P.; Rispoli, F.; Paris, E.; Carnevale, M.; Colantoni, A. Influence of Oxidant Agent on Syngas Composition: Gasification of Hazelnut Shells through an Updraft Reactor. *Energies* **2020**, *13*, 102. [[CrossRef](#)]
33. Littlewood, K. Gasification: Theory and application. *Prog. Energy Combust. Sci.* **1977**, *3*, 35–71. [[CrossRef](#)]
34. Aghaalikhani, A.; Savuto, E.; Di Carlo, A.; Borello, D. Poplar from phytoremediation as a renewable energy source: Gasification properties and pollution analysis. *Energy Procedia* **2017**, *142*, 924–931. [[CrossRef](#)]
35. Paris, E.; Carnevale, M.; Vincenti, B.; Palma, A.; Guerriero, E.; Borello, D.; Gallucci, F. Evaluation of VOCs Emitted from Biomass Combustion in a Small CHP Plant: Difference between Dry and Wet Poplar Woodchips. *Molecules* **2022**, *27*, 995. [[CrossRef](#)]

**Disclaimer/Publisher’s Note:** The statements, opinions and data contained in all publications are solely those of the individual author(s) and contributor(s) and not of MDPI and/or the editor(s). MDPI and/or the editor(s) disclaim responsibility for any injury to people or property resulting from any ideas, methods, instructions or products referred to in the content.